Measurement of T_2 and T_2* in Spin Echo Single Point EPR Imaging Using a Single Acquisition Method

Hyungseok Jang[1], Sankaran Subramanian[2], Nallathamby Devasahayam[2], Shingo Matsumoto[2], Keita Saito[2], Murali C. Krishna[2], and Alan B. McMillan[1]

[1]*Radiology, University of Wisconsin, Madison, WI, United States,* [2]*Radiation Biology Branch, Center for Cancer Research, NCI, National Institutes of Health, Bethesda, MD, United States*

Target Audience Researchers interested in quantitative oxygen imaging using electron paramagnetic resonance imaging.

Purpose Electron paramagnetic resonance imaging (EPRI) has surfaced as a promising technique that can allow quantitative imaging of tissue oxygenation. Owing to the extremely short spin-spin relaxation time of the spin probe (Oxo63), current EPRI benefits from single point imaging (SPI) scheme where entire FID is phase encoded under static phase encoding gradients[1]. Several methods have been proposed to overcome zoom-in effect (time-decreasing FOV) resulting from using static phase encoding gradients and thereby enable direct T_2*/pO_2 estimation, such as the multiple acquisition method[2], a single acquisition method[3], and a spin echo-based method[4]. Among the techniques, spin echo based SPI-EPRI (ESPI-EPRI) is worthy of study because it can allow simultaneous T_2 and T_2* estimation when combined with a single acquisition method. In EPRI, T_2/T_2* parameters are used as a precursor to pO_2 quantification owing to their inversely proportional relation. In this study, the physical and physiological significance of T_2 and T_2* measures was explored through ESPI-EPRI.

Methods To obtain images with an equal FOV in ESPI, we extended a single acquisition method using gridding and k-space extrapolation (KSE)[3]. Since there are three independent segments in ESPI as seen in Fig. 1-a, KSE can be applied in two different ways, intra-segment or inter-segment extrapolation. In intra-segment KSE, k-spaces are extrapolated independently within each segment as shown in Fig. 1-b, whereas inter-segment KSE benefits from k-spaces in different segments as shown in Fig. 1-c. Once equal FOV images have been secured, T_2 and T_2* can be fit over a large amount of data points (typically 100-300 points) using the following piecewise signal equation:

$$M = M_0 \exp\left(-\frac{t}{T_2}-\frac{t}{T_2'}\right) \quad \text{for } t < \text{TE}/2$$

$$M = M_0 \exp\left(-\frac{t}{T_2}-\frac{t-TE}{T_2'}\right) \quad \text{for TE}/2 \le t < \text{TE}$$

$$M = M_0 \exp\left(-\frac{t}{T_2}-\frac{TE-t}{T_2'}\right) \quad \text{for } t > \text{TE}$$

, where TE denotes echo time. T_2 and T_2' can be directly fit if TE is known, and T_2* can be calculated by the equation, T_2* = 1/(1/T_2+1/T_2'). We compared quantitative measurements of single acquisition ESPI and single acquisition FID-SPI on a 10 mT EPR scanner[1].

Results Inter-segment KSE (Fig. 1d-bottom) yields better imaging quality than intra-segment (Fig. 1d-top) because error propagated during extrapolation is alleviated by taking data from the first segment that has higher SNR. Fig. 2a shows the T_2* map estimated by applying single acquisition FID-SPI, and Fig. 2b and Fig. 2c show the T_2* map and T_2 map estimated using the proposed method with ESPI data, respectively. Table 1 shows estimated T_2/T_2* in each tube and the resultant %O_2-$R_{2(*)}$ curve fits.

Discussion and Conclusion A new approach for single acquisition quantitative ESPI has been presented. As shown in Table 1, similar estimates of T_2* were obtained between FID and ESPI approaches. While the observed T_2 is significantly larger (as expected), the slope of T_2 and T_2* with varying oxygenation is very similar, indicating similar sensitivity to oxygenation with either parameter. Future work is needed to evaluate the physiological significance between T_2 and. T_2* measurements for *in vivo* tumor hypoxia imaging. Further, tradeoffs between the value of SPI, which offers a shorter TR and thus more rapid imaging, versus ESPI which allows estimation of both parameters and a higher intrinsic SNR should be examined.

References

1. Subramanian et al. (2002). MRM. 48: 370–379. **2.** Matsumoto et al. (2006). MRM. 55: 1157-1163. **3.** Jang et al. (2013). MRM. 00: 1–9. **4.** Subramanian et al. (2012). JMR. 218: 105-114

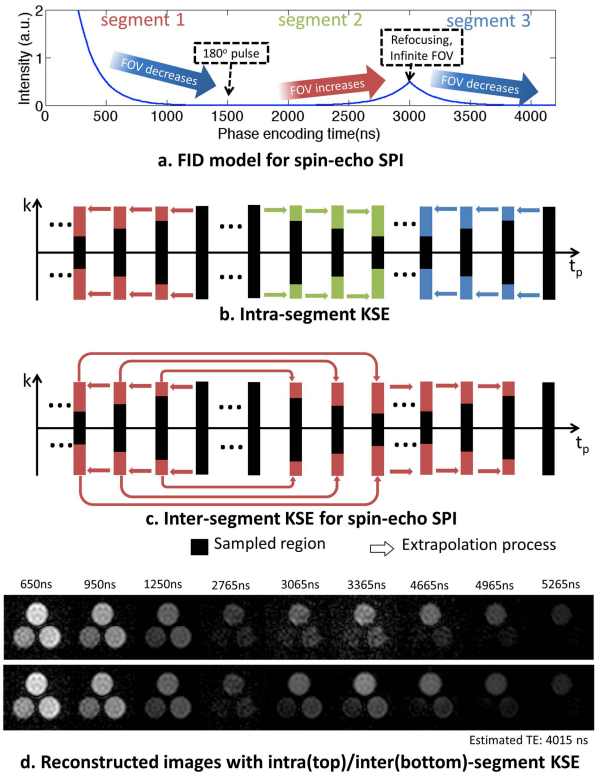

Figure 1. k-space extrapolation in ESPI.

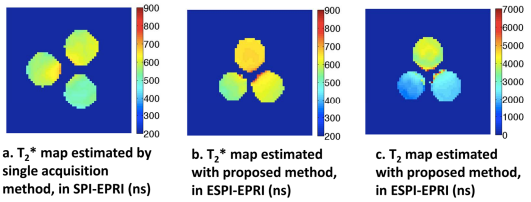

Figure 2. Estimated T_2* maps. 19x19x19 SPI data was used for a, and 21x21x21 ESPI data was used for b. 2D slices are shown.

	T_2/T_2*(ns)			%O_2-$R_{2(*)}$ curve fit		
	Tube 1 (0%)	Tube 2 (2%)	Tube 3 (5%)	Slope (1/ns%O_2)	Y-intercept (1/ns)	R^2
SPI (T_2*)	625.7 ± 69.2	600.4 ± 48.9	534.9 ± 41.4	5.15 x10^{-5}	1.61x10^{-3}	0.99
ESPI (T_2*)	673.9 ± 57.7	620.7 ± 22.8	572.8 ± 41.0	5.28 x10^{-5}	1.49x10^{-3}	0.99
ESPI (T_2)	4219.4 ± 334.2	2329.1 ± 184.6	1939.5 ± 258.6	5.14x10^{-5}	2.87x10^{-4}	0.96

Table 1. Estimated parameters. A 3-tube phantom of Oxo 63 bubbled with of 0%, 2%, 5% oxygen was used.